Human mesenchymal stem cells exert potent antitumorigenic effects in a model of Kaposi's sarcoma

Aarif Y. Khakoo,[1,9] Shibani Pati,[6,7] Stasia A. Anderson,[5] William Reid,[6,7] Mohamed F. Elshal,[2] Ilsa I. Rovira,[1] Ahn T. Nguyen,[6,7] Daniela Malide,[3] Christian A. Combs,[3] Gentzon Hall,[8] Jianhu Zhang,[9] Mark Raffeld,[4] Terry B. Rogers,[8] William Stetler-Stevenson,[4] Joseph A. Frank,[5] Marvin Reitz,[6,7] and Toren Finkel[1]

[1]Laboratory of Molecular Biology, Cardiovascular Branch, [2]Flow Cytometry Core Facility, and [3]Light Microscopy Core Facility, National Heart, Lung, and Blood Institute; [4]National Cancer Institute; and [5]Experimental Neuroimaging Section, Laboratory of Diagnostic Radiology Research, National Institutes of Health, Bethesda, MD 20892
[6]Institute of Human Virology, University of Maryland Biotechnology Institute, [7]Department of Microbiology and Immunology, and [8]Department of Biochemistry, School of Medicine, University of Maryland, Baltimore, MD 21201
[9]Department of Cardiology, The University of Texas MD Anderson Cancer Center, Houston, TX 77030

Emerging evidence suggests that both human stem cells and mature stromal cells can play an important role in the development and growth of human malignancies. In contrast to these tumor-promoting properties, we observed that in an in vivo model of Kaposi's sarcoma (KS), intravenously (i.v.) injected human mesenchymal stem cells (MSCs) home to sites of tumorigenesis and potently inhibit tumor growth. We further show that human MSCs can inhibit the in vitro activation of the Akt protein kinase within some but not all tumor and primary cell lines. The inhibition of Akt activity requires the MSCs to make direct cell–cell contact and can be inhibited by a neutralizing antibody against E-cadherin. We further demonstrate that in vivo, Akt activation within KS cells is potently downregulated in areas adjacent to MSC infiltration. Finally, the in vivo tumor-suppressive effects of MSCs correlates with their ability to inhibit target cell Akt activity, and KS tumors engineered to express a constitutively activated Akt construct are no longer sensitive to i.v. MSC administration. These results suggest that in contrast to other stem cells or normal stromal cells, MSCs possess intrinsic antineoplastic properties and that this stem cell population might be of particular utility for treating those human malignancies characterized by dysregulated Akt.

The Journal of Experimental Medicine

CORRESPONDENCE
Aarif Y. Khakoo:
aykhakoo@mdanderson.org

Abbreviations used: HUVEC, human umbilical vein endothelial cell; KS, Kaposi's sarcoma; MRI, magnetic resonance imaging; MSC, mesenchymal stem cell; VEGF, vascular endothelial growth factor.

Work over the past 30 yr has resulted in a greater understanding of the biology and therapeutic application of human stem cells in human malignancies. The use of stem cell transplantation is an important tool in the treatment of several hematologic (1) and nonhematologic (2, 3) malignancies. In contrast, several recent studies have suggested that stem and progenitor cells may be direct cellular targets of the genetic alterations leading to tumor formation as well as important contributors to the maintenance of human cancers (4–6). In addition, other recent studies have altered the perception of the stromal cells that surround epithelial tumors from being innocent bystanders in the neoplastic process to being a cell type that actively promotes the growth of the adjacent transformed cells (7–11). However, the effect of human mesenchymal stem cells (MSCs), the stromal progenitor stem cells found within the bone marrow, on the growth of human tumors is not well understood.

The cell population known as MSCs are usually isolated from the mononuclear fraction of a bone marrow aspirate, which is then depleted of $CD45^+$ cells and subsequently isolated as the cell population that adheres to plastic tissue culture dishes (12). MSCs can proliferate for many passages in culture and have the ability to give rise to several differentiated cell types (13). MSCs have several properties that make them an attractive choice as a cell therapeutic

A.Y. Khakoo and S. Pati contributed equally to this paper.
The online version of this article contains supplemental material.

agent (14). They are easily obtained from a simple bone marrow aspirate that can be readily expanded to hundreds of millions of cells. MSCs also appear to have the ability to home to sites of tissue injury (15, 16). MSCs are easily transfectable, allowing for easy ex vivo modification. Finally, MSCs appear to be relatively nonimmunogenic (17), although the mechanism of their immune privilege is not well understood and is a subject of intense study (18, 19).

Because of these properties, MSCs have considerable therapeutic potential in several disease processes, including cardiovascular disease (20), as well as in the treatment of human malignancies (21). To explore the role of MSCs on tumorigenesis, we studied the effects of human MSCs on Kaposi's sarcoma (KS), a highly inflammatory angiogenic tumor. KS is the most common AIDS-related malignancy (22, 23) and is characterized by multiple cutaneous and visceral vascular lesions in affected patients. Propagation of KS is dependent on proinflammatory cytokines, angiogenic factors, and adhesion molecule expression, all of which promote KS pathogenesis through both paracrine and autocrine mechanisms (24). The production of many of these components is initiated by human herpes virus 8 infection, a necessary factor in KS pathogenesis (25, 26).

Based on the previous studies implicating stem cells and stromal support cells in the neoplastic process (4–11), we anticipated that transplanted MSCs would accelerate the growth of tumors in vivo. In fact, some studies suggest that MSCs may represent a precursor to tumorigenic cells (27, 28). In addition, another study suggests that through their immune suppressive effects, transplanted MSCs may enhance tumor growth in vivo (19). Furthermore, MSCs produce proangiogenic cytokines and have been shown to enhance blood vessel growth in several studies of chronic limb ischemia (29–31). Surprisingly, as described in this study, we found that MSCs can instead exert a profound antitumorigenic effect that appears to be mediated by a contact-dependent inhibition of Akt activity.

RESULTS

i.v. injected human MSCs home to KS tumors in vivo

Human MSCs were obtained from several young, healthy donors and were pooled for use in all experiments. We extensively characterized these cells to show that they expressed the characteristic cell surface markers and produced the cytokines typical of human MSCs (see Figs. S1 and S2, available at http://www.jem.org/cgi/content/full/jem.20051921/DC1). In particular, we observed that human MSCs produce high levels of proangiogenic cytokines in vitro.

Because previous studies have suggested that mature stromal cells promote tumorigenesis through local paracrine effects (8, 9), we found it necessary to determine whether i.v. injected human MSCs could home to KS tumors in vivo. Previous studies suggest that systemically infused MSCs have the ability to home to sites of active tumorigenesis (21, 32). To test this in our model, on day 0, 4×10^6 human MSCs were injected i.v. into the tail vein of an athymic nude mouse. On the same day, 5×10^6 KS cells were implanted subcutaneously into the right flank of the same mouse. To track the distribution of the MSCs within the mouse over time, we labeled the MSCs with superparamagnetic iron oxide particles, which allows for in vivo tracking of the cells by magnetic resonance imaging (MRI) by producing a characteristic hypointense area resulting in a signal void within the MRI image. A similar approach has been previously demonstrated to effectively track the in vivo location of MSCs without the alteration of cellular function (33, 34). We also labeled the MSCs with a conjugated fluorophore (CM-DiI) to allow for easy identification in histopathological sections.

MRI of the subcutaneous flank tumor demonstrated evidence for the localization of iron oxide–labeled MSCs, which were indicated by small focal hypointense areas around the tumor (Fig. 1 A). These effects were observed as early as 48 h after tumor implantation. Labeled MSCs were imaged with ~100-μm in-plane resolution and 350-μm slice thickness. Over time, the hypointense MRI effect became more pronounced at the tumor periphery (Fig. 1 A). We also performed total body MRI of mice at 50-μm resolution in three dimensions to evaluate all of the major organs and bone marrow (Fig. S3, available at http://www.jem.org/cgi/content/full/jem.20051921/DC1). In both tumor-bearing and non–tumor-bearing mice, we only observed extensive regions of a signal void, which are indicative of labeled MSCs, in the reticuloendothelial system and within the lungs. We did not observe appreciable numbers of MSCs in other highly vascular tissues, including the heart, brain, kidney, and skeletal muscle.

To confirm that the MRI findings represented the presence of iron-labeled MSCs within the tumors, we examined the excised tumors with fluorescence microscopy to look for the presence of the red fluorochrome CM-DiI. At day 2, labeled MSCs were seen diffusely distributed throughout the densely cellular KS tumor (Fig. 1 B). At higher magnification, MSCs within KS tumors appeared to maintain the elongated, fibroblast-like appearance that they adopt in culture (Fig. 1 C). At day 5, we still could observe numerous MSCs within the center of the tumor, particularly around what appeared to be acellular and necrotic areas (Fig. 1 D). By day 7, the overall number of MSCs within the tumor had diminished by almost threefold (day 2 vs. day 7; 47 cells/high power field ± 11 vs. 17 cells/high power field ± 10; $P < 0.001$; $n = 3$ for each group). MSC homing to KS tumors maintained the spindle-shaped morphology that they adopted in culture, and these CM-DiI–positive cells showed no evidence of differentiation along myeloid or hematopoietic cell lineages, as assessed by the lack of expression of CD33, CD34, and myeloperoxidase, whereas the vast majority of MSCs maintained the expression of CD44 (unpublished data).

Human MSCs inhibit the growth of KS tumors in a dose-dependent manner

We next sought to assess the effects of i.v. injected human MSCs on in vivo KS tumor growth. Surprisingly, as demonstrated in Fig. 2 A, a single dose of 4×10^6 MSCs that

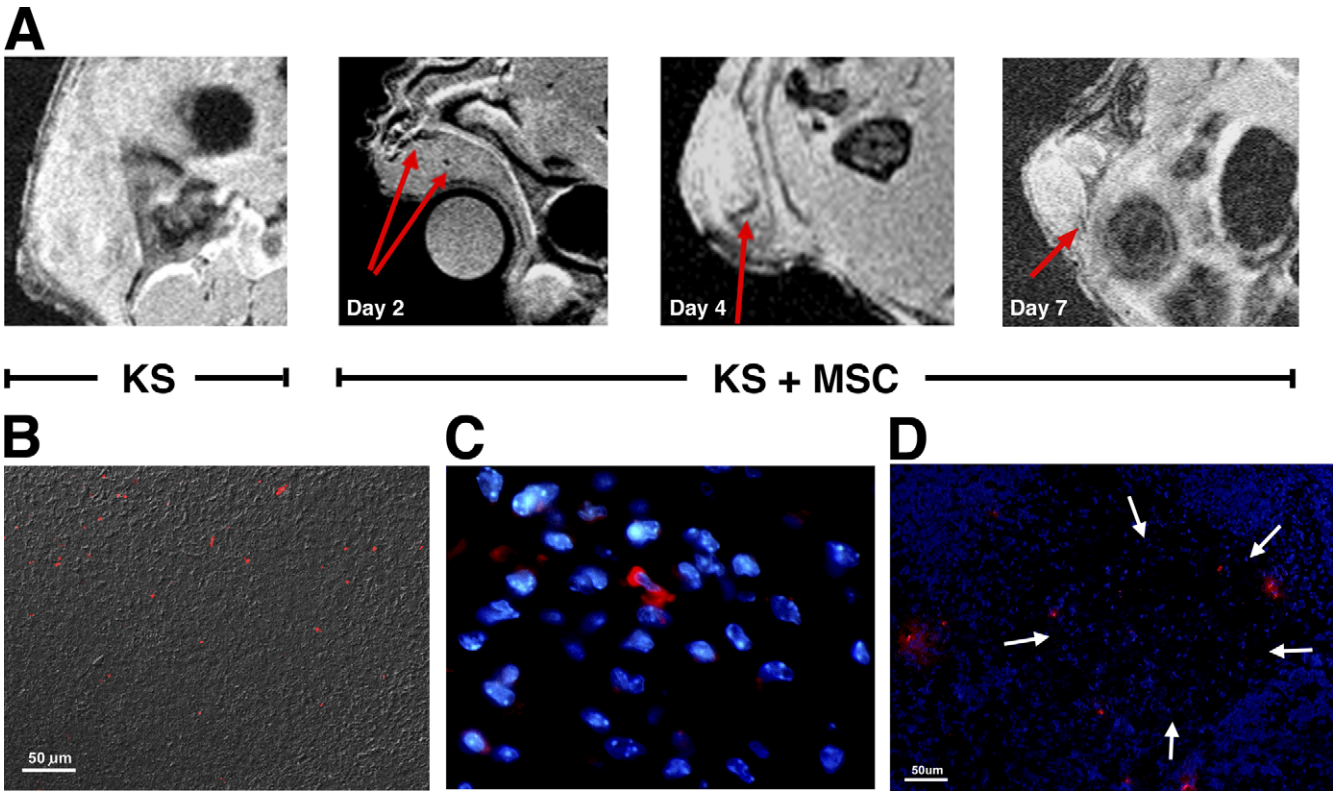

Figure 1. i.v. administered human MSCs home to KS tumors in vivo. Human MSCs were labeled with both superparamagnetic iron nanoparticles and the red fluorochrome CM-DiI. Where indicated, 4×10^6 labeled MSCs were injected into the tail vein of an athymic nude mouse. On the same day, 5×10^6 KS cells were injected subcutaneously into the posterior right flank. (A) MRI imaging reveals that as early as 2 d after i.v. injection, iron-labeled MSCs can be identified within the KS tumors, as indicated by the signal void created by the iron-containing MSCs within the KS tumor (arrows). Cells are seen prominently within the body of the tumor on day 4 (arrow). By day 7 after cell injection, a minimal signal void is observed at the periphery of a tumor (arrow). (B) On day 2, MSCs are diffusely distributed within the tumor, as indicated by a low power epifluorescence image superimposed on a phase-contrast photomicrograph. (C) High power epifluorescence image of a single red CM-DiI–labeled human MSC residing within a day 4 KS tumor. Cell nuclei are stained using a blue fluorescent DAPI counterstain. (D) Multiple CM-DiI–labeled MSCs within a day 4 KS tumor surround a relatively acellular, circular necrotic area within the tumor (arrows).

was administered i.v. coincident with KS tumor implantation resulted in a >50% decrease in KS tumor size (Fig. 2 A). Analysis of mean (Fig. 2 B) and individual tumor growth curves demonstrates the robustness of this effect (Fig. 2 C). To determine whether the observed effect on KS tumorigenesis represented a nonspecific response to i.v. injection of human cells in our athymic nude mouse model of KS, we performed similar experiments using infused human umbilical vein endothelial cells (HUVECs), which express similar levels of MHC class I and II compared with human MSCs (unpublished data). As noted in Fig. 2 D, we found that i.v. injection of HUVECs had no significant ($P = 0.47$) effect on KS tumorigenesis.

Our in vivo tracking results (Fig. 1) suggested that there is a significant reduction ($P < 0.001$) of the number of MSCs at the tumor site over the first 7 d. Therefore, we reasoned that multiple i.v. dosages of human MSCs could potentially augment the observed inhibition of KS tumorigenesis. Consistent with this hypothesis, i.v. administration of 4×10^6 human MSCs on days 0, 3, and 10 significantly ($P < 0.001$) augmented the in vivo inhibition of KS tumor growth when compared with a single dose of human MSCs (Fig. 2 E). In contrast, as seen in Fig. 2 E, multiple dosages of HUVECs had no significant effect ($P = 0.79$) on KS tumorigenesis.

In the aforementioned experiments, MSCs were routinely injected on the same day that KS tumors were initiated. Because tumor establishment and subsequent tumor growth are distinct biological processes, we sought to determine whether human MSCs exerted similar antitumorigenic effects in animals with preestablished KS tumors. To test this, 3×10^6 KS cells were inoculated in the right flank on day 0. Palpable tumors were appreciated in all animals by day 7. A subset of animals was then treated with 3×10^6 human MSCs on days 7, 13, and 17. 4 d after i.v. injection, CM-DiI–labeled human MSCs were identified diffusely throughout these preexisting tumors (unpublished data). Serial analysis of these animals for >1 mo after tumor implantation demonstrated that human MSCs also significantly inhibited KS tumor growth ($P < 0.05$) in animals with preestablished tumors (Fig. 2 F).

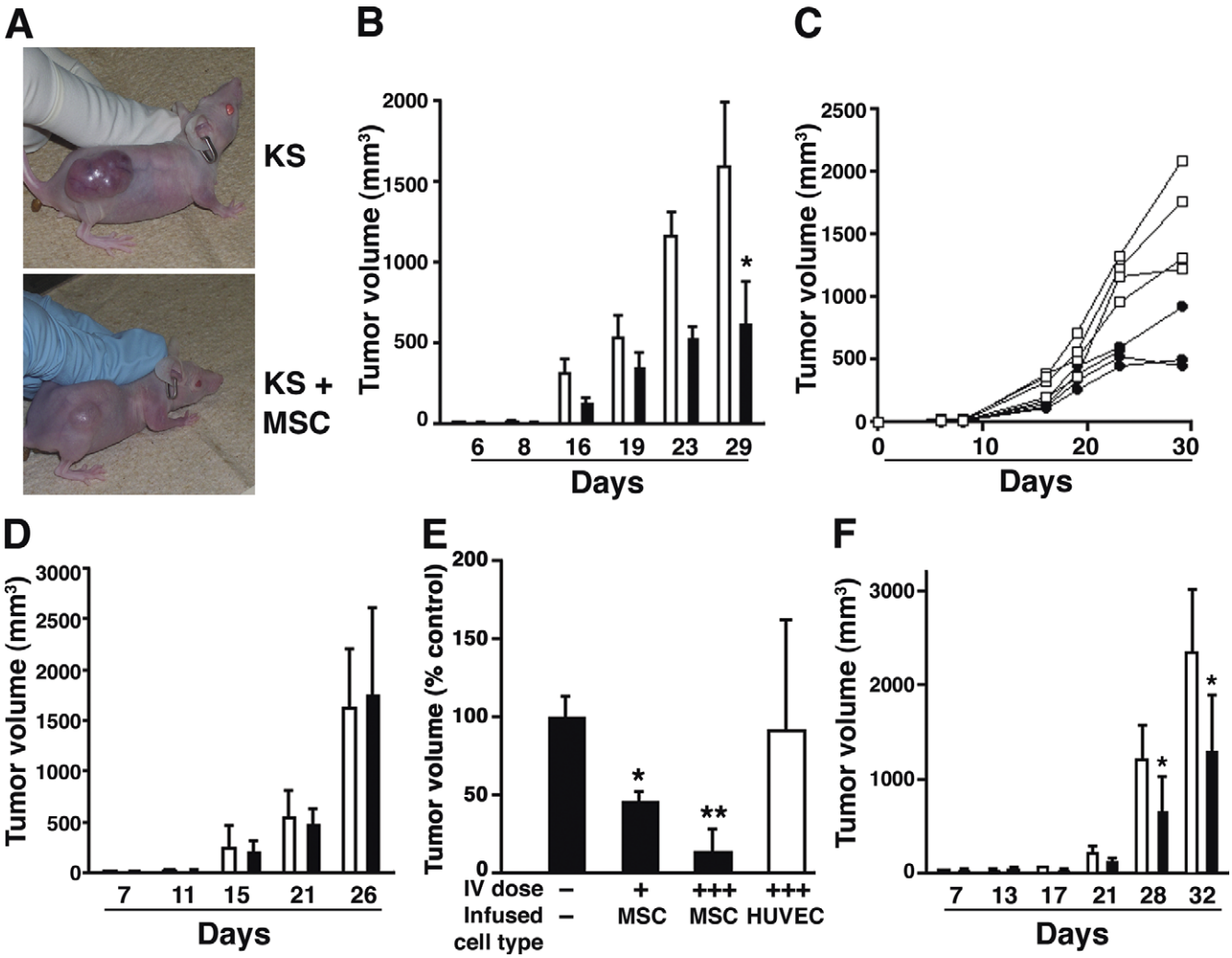

Figure 2. i.v. administered MSCs inhibit KS tumorigenesis in vivo. (A) Representative tumors on day 23 in athymic nude mice receiving no treatment (KS) or receiving a single i.v. dose of 4×10^6 MSCs (KS + MSC). (B) On day 0, 5×10^6 KS cells were injected subcutaneously into the posterior right flank of each mouse alone (white bars) or in conjunction with i.v. administration of 4×10^6 human MSCs (black bars). Tumor growth and progression were monitored by biweekly caliper assessment (*, $P < 0.005$ on day 29; $n = 4$ per group). Data shown is from one experiment that is representative of results from three similar experiments. (C) Individual tumor growth curves from mice receiving a single dose of i.v. MSCs (circles) compared with growth curves from untreated animals (squares). (D) Similar design as in B except that animals received KS cells alone (white bars) or, on day 0, the simultaneous i.v. delivery of 4×10^6 HUVECs (black bars; P value is NS at day 26; $n = 6$ for each group). (E) Reduction in tumor volume for animals receiving multiple doses (+ + +) of 4×10^6 MSCs i.v. on days 0, 3, and 10 versus a single dose (+) of i.v. MSCs on day 0 (*, $P < 0.005$; $n = 6$ per group; single dose of MSCs vs. untreated animals; **, $P < 0.001$; $n = 6$ per group; single dose of MSC treatment vs. multiple dosages of MSC treatment). In contrast, animals receiving multiple doses of 4×10^6 HUVECS i.v. on days 0, 3, and 10 were indistinguishable from animals receiving KS cells alone. Data is expressed as the percentage of day 23 tumor volume with animals that received KS cells alone set at 100%. (F) Mean tumor volume in animals with preexisting tumors. All animals had palpable, well-established tumors before the administration of the first dosage of MSCs and were randomized to receive saline infusion or multiple doses of 4×10^6 MSCs i.v. on days 7, 13, and 17 (*, $P < 0.05$; $n = 6$ in the treated group; $n = 4$ in the untreated group). Error bars represent SEM.

Coculture of human MSCs with KS cells inhibits activation of Akt within KS cells in a contact-dependent manner

To understand the mechanism of the in vivo inhibition of KS tumor growth by i.v. injected MSCs, we performed a series of KS cell/MSC coculture experiments. In normal growth media, KS cell proliferation was not affected by coculturing with MSCs (Fig. 3 A). Similarly, coculture of MSCs with KS cells had no effect on vascular endothelial growth factor (VEGF) promoter activity within KS cells or overall VEGF secretion by KS cells (unpublished data). Because in vitro culture conditions do not faithfully reproduce the tumor microenvironment (35, 36), we asked whether in vitro KS proliferation might be altered by MSCs under conditions of diminished nutrient supply. When KS cells were cultured independently of MSCs, there was no difference in the growth rate of these cells in full growth media when compared with

growth in media with moderately reduced extracellular glucose (Fig. 3 B). In contrast, as seen in Fig. 3 B, the growth of KS cells cocultured with MSCs was significantly reduced when grown in the presence of media with lower glucose. Similar results were obtained in media containing reduced FCS (unpublished data). Importantly, when MSCs and KS cells were cocultured but separated by a transwell membrane, which allows the exchange of soluble factors but prevents direct cell–cell contact, KS proliferation was not affected by altering glucose levels (Fig. 3 B).

To further explore the effect of human MSCs on KS cells, we next examined the effects of MSCs on activation of the protein kinase Akt, which is a critical mediator of KS tumor growth and survival. Inhibition of Akt activity by the pharmacologic blockade of the upstream activator PI3 kinase or genetic suppression by the expression of a dominant-negative Akt construct has been previously shown to result in the profound inhibition of KS cells (37). These results suggest an important physiologic link between Akt activation and KS cell survival. In addition, in a mouse KS model, pharmacological inhibition of Akt has been shown to inhibit tumorigenesis (38). Given the importance of this pathway to KS biology, we asked whether direct coculture with MSCs inhibited Akt activation in KS cells.

To test this hypothesis, we made use of the fact that after direct coculture, the KS cell population could be repurified by flow cytometry based on both size and cell surface characteristics of KS cells (Fig. 3 C). As demonstrated in Fig. 3 D, when KS cells were repurified after direct MSC coculture, we observed a potent decrease in the levels of Akt phosphorylation (serine position 473). Similar results were obtained using an antibody that recognizes phosphothreonine at position 308 of Akt (unpublished data). In contrast, as seen in Fig. 3 E, total Akt levels were unaffected by coculture. Notably, the inhibitory effect on Akt phosphorylation was not seen when KS cells were directly cocultured with mature endothelial cells (Fig. S4, available at http://www.jem.org/cgi/content/full/jem.20051021/DC1). Similar to the effects of MSCs on KS proliferation, when MSCs and KS cells were cocultured but separated by a transwell membrane, the inhibition of Akt phosphorylation within KS cells was not observed (Fig. 3 F). These effects appeared specific because the direct coculture of MSCs and KS cells did not alter the levels of either phosphorylated ERK1/2 or phosphorylated MEK1/2 within KS cells (Fig. 3 G and Fig. S5). Together, these findings demonstrate that MSCs specifically inhibited Akt activation within KS cells and that this interaction requires direct cell contact.

Several groups have observed that the immunosuppressive effects of human MSCs are mediated by the effects of MSCs on antigen-presenting cells (39, 40) and that these effects require (39) direct cell contact or are potentiated by direct cell contact (40). Collectively with our findings, this suggests a potent biological activity of human MSCs affecting a variety of cell types occurring only when the two cell types are in close contact. Because adhesive cell–cell interactions are mediated by cadherin proteins and because the loss of expression of the cell surface protein E-cadherin promotes a more aggressive phenotype of transformed cells in vitro and in vivo (41–44), we asked whether treatment with a neutralizing antibody against E-cadherin could block the effect of MSCs on KS cells. As noted in Fig. 3 H, the addition of a neutralizing antibody to E-cadherin to MSC/KS cocultures markedly attenuated the inhibitory effects of MSCs on Akt activation within KS cells (compare with Fig. 3 D). We observed no effect on Akt activity in these cultures after the addition of an isotype IgG control antibody. These findings further support the requirement of direct cell–cell contact in mediating the effects of MSCs on target cells.

Human MSCs inhibit Akt activation within other primary cell lines but not within other tumor cell lines

To further explore the effects of MSCs on target cell Akt activation within cell types other than KS cells, we directly cocultured human MSCs with two different primary cell lines and with two different tumor cell lines. Direct coculture of human MSCs with either a primary endothelial cell culture (Fig. 4 A) or with primary neonatal cardiac myocytes (Fig. 4 B) substantially inhibited phospho-Akt levels without affecting total Akt levels. The latter result is of particular interest given the observed inhibition of pathological cardiac hypertrophy in animals treated with MSCs after myocardial infarction (45, 46) and the well-established link between Akt activation and hypertrophy in cardiac myocytes (47, 48). As previously seen in KS/MSC cocultures, transwell culture of human MSCs with primary endothelial cells had no effect on phospho-Akt levels within the endothelial cells (unpublished data). Similarly, treatment of MSC/endothelial cell cocultures with a neutralizing antibody against E-cadherin abrogated the inhibition of Akt activation within endothelial cells (Fig. 4 C). In contrast to these effects, incubation of MSCs with the prostate tumor cell line PC-3 or the breast cancer tumor line MCF-7 had no effect on phospho-Akt levels within PC-3 cells (Fig. 4 D) or MCF-7 cells (not depicted).

Antitumorigenic effect of human MSCs requires the inhibition of Akt activation within tumor target cells

We then asked whether the in vivo effects of MSCs on KS tumorigenesis are linked to the inactivation of Akt within KS target cells. 2 d after the simultaneous i.v. injection of MSCs and subcutaneous implantation of KS tumors, tumors were harvested and lysed. Western blot analysis revealed that compared with tumors from animals that received no human MSCs, KS tumors from animals receiving MSCs had decreased levels of phosphorylated Akt (Fig. 5 A). To assess whether known Akt targets were also reduced in the KS tumors, we analyzed the phospho– to total GSK-3β ratio from tumor lysates in control animals as well as those animals receiving MSCs. Consistent with the observed reduction in phospho-Akt, we noted an ~25% reduction in phospho–GSK-3β activity in animals receiving coadministered MSCs (phospho–GSK-3β/total GSK-3β ratio in arbitrary units:

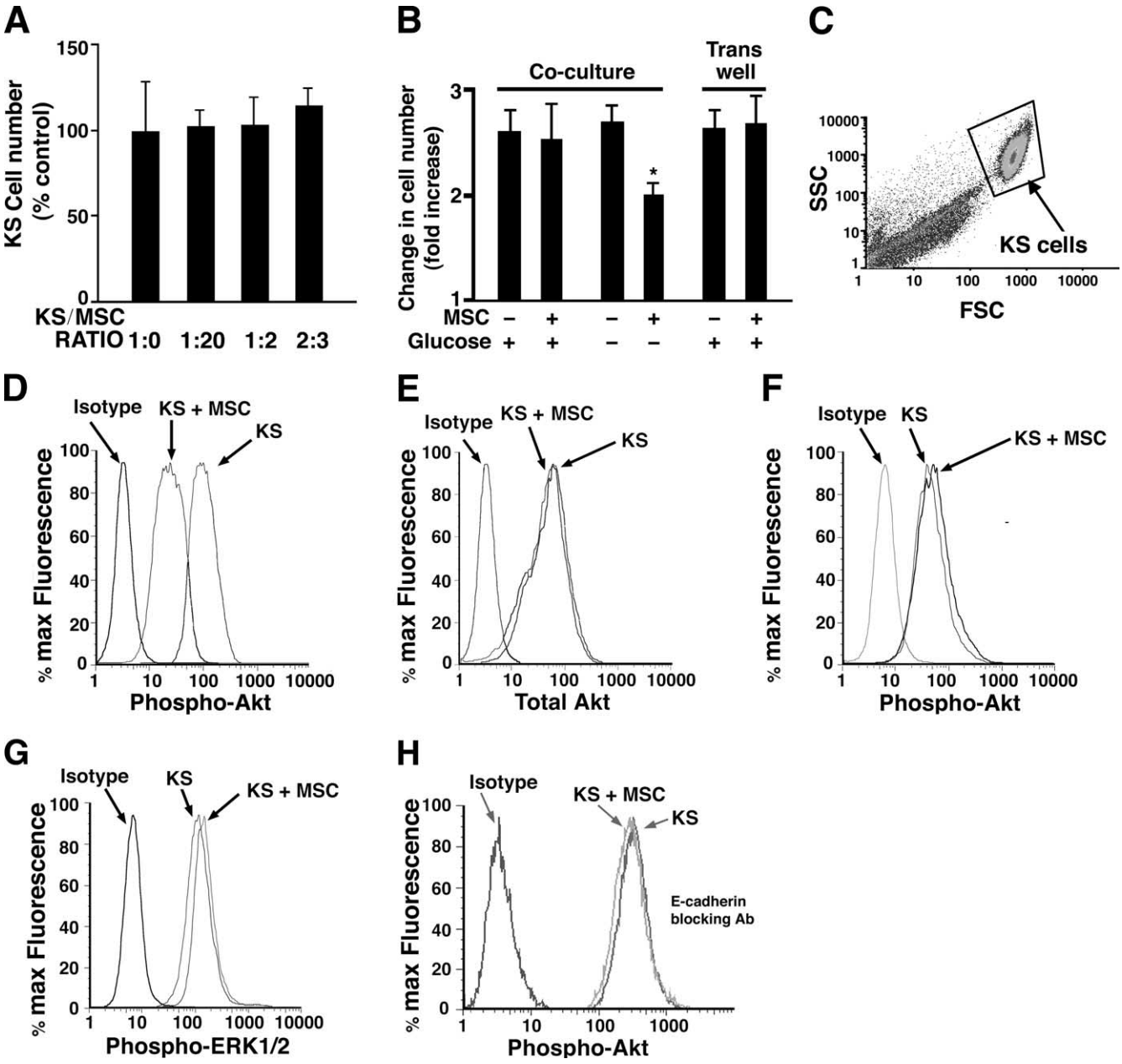

Figure 3. MSCs induce a contact-dependent inhibition of Akt activation. (A) The proliferation of KS cells is not affected by direct coculture with MSCs in full growth media. Various ratios of KS cells to MSCs are shown. (B) Change in cell number over 48 h of KS cells grown in the presence or absence of MSCs and cultured with either 2 g/liter (+) or 1 g/liter (−) glucose. KS cell growth was assessed with MSCs in a coculture format as well as in a transwell format, which prevented KS–MSC cell contact. *, $P < 0.005$. (C) KS cells were cocultured with MSCs for 18 h in a 1:10 (MSC/KS cell) ratio. Flow cytometric forward scatter and side scatter analysis of KS cell–MSC cocultures demonstrating the separation of viable, larger KS cells from human MSCs. Cell surface staining for Stro-1, a marker present on most human MSCs but not on KS cells, was used to further gate out MSCs (not depicted). (D) Levels of phosphorylated Akt (Ser473) in KS cells directly cocultured with MSCs (KS + MSC) were reduced compared with levels of phosphorylated Akt in KS cells alone (KS). (E) Total Akt levels within KS cells are not affected by coculture with MSCs. (F) No difference in phosphorylated Akt levels were seen in KS cells cocultured with MSCs but separated by a transwell (KS + MSC) compared with KS cells alone (KS). (G) Levels of phosphorylated ERK1 and 2 (Thr202 and Tyr204 combined) were not significantly affected by direct coculture with MSCs (KS + MSC) compared with KS cells alone. (H) KS cells were directly cocultured with MSCs for 18 h in a 1:10 (MSC/KS cell) ratio in the presence of a blocking antibody against E-cadherin. The inhibitory effects of MSCs on Akt phosphorylation in KS cells are markedly reduced in the presence of a neutralizing antibody against E-cadherin (compare with D). All of the aforementioned results are representative of at least three similar experiments. Error bars represent SEM.

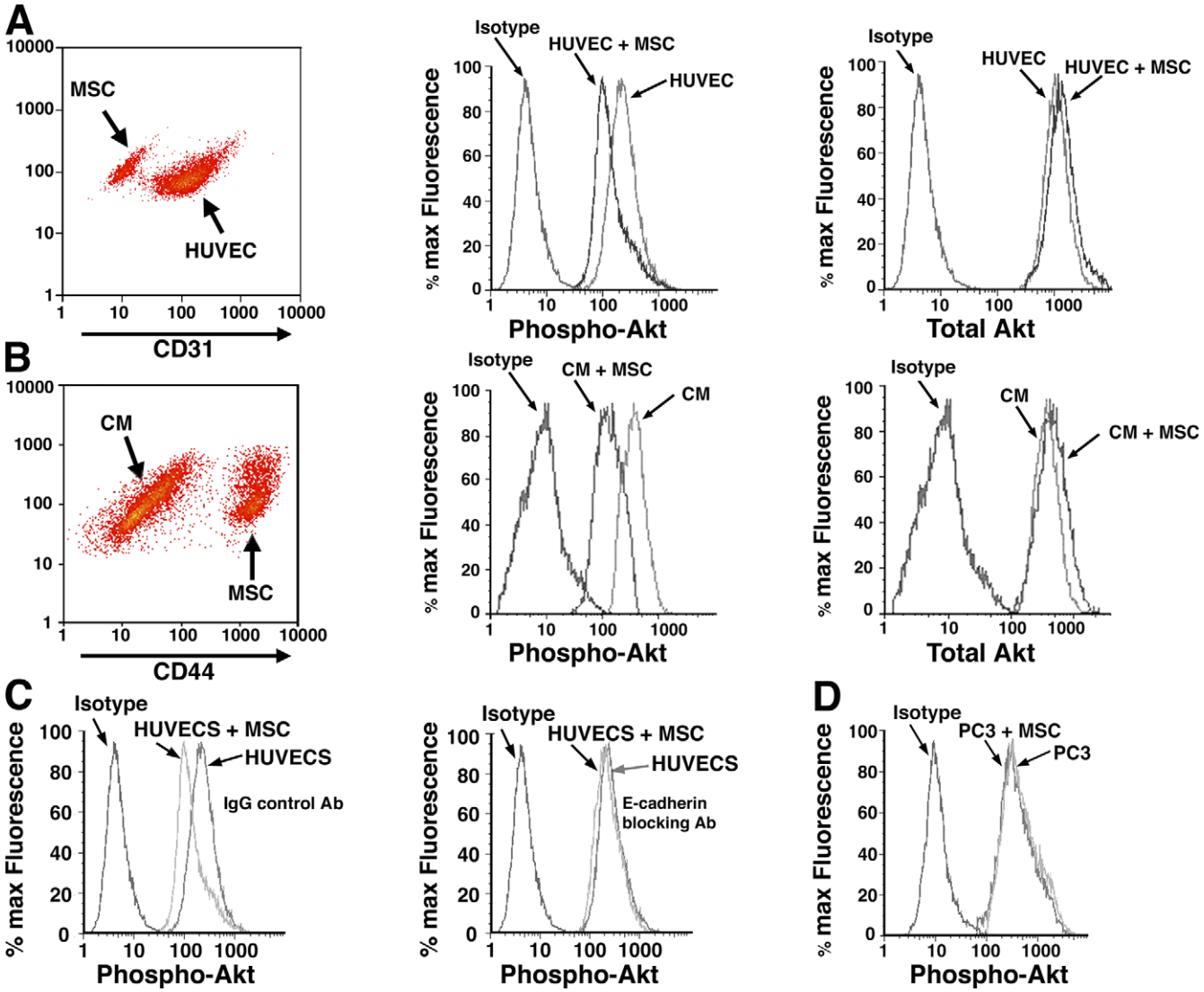

Figure 4. Akt activation within cardiac myocytes and mature endothelial cells but not prostate tumor cells is inhibited by coculture with MSCs. Neonatal cardiac myocytes (CM), HUVECs, or PC-3 cells were cocultured with human MSCs at a ratio of 1:10 (MSC/target cell). 18 h after coculture, phospho-Akt levels within cardiac myocytes, HUVECs, or PC-3 cells were assessed by flow cytometry and compared with phospho-Akt levels with cardiac myocytes, HUVECs, or PC-3 cells cultured alone. (A) In MSC/HUVEC cocultures, HUVECs were repurified using an antibody against human CD31 (left). Levels of phosphorylated Akt (Ser473) in HUVECs directly cocultured with MSCs (HUVEC + MSC) are decreased compared with HUVECs cultured alone (middle). Total Akt levels in HUVECS are unchanged in the presence of MSCs compared with HUVECs cultured alone (right). (B) In MSC/cardiac myocyte cocultures, MSCs were gated out using an antibody against human CD44, which reacts with human MSCs but not mouse neonatal cardiac myocytes (left). Levels of phosphorylated Akt (Ser473) in cardiac myocytes directly cocultured with MSCs (CM + MSC) are decreased compared with cardiac myocytes cultured alone (CM; middle). Total Akt levels in neonatal cardiac myocytes are unchanged in the presence of MSCs compared with cardiac myocytes cultured alone (right). (C) MSCs were cocultured with HUVECs for 18 h in a 1:10 (MSC/HUVEC) cell ratio in the presence of a blocking antibody against E-cadherin or an IgG control antibody. The inhibitory effects of MSCs on Akt phosphorylation in KS cells seen in the presence of control IgG antibody (left) are abrogated in the presence of a neutralizing antibody against E-cadherin (right). (D) PC-3 cells were cocultured with MSCs for 18 h in a 1:10 (MSC/PC-3) cell ratio. Cell surface staining for prostate cell surface antigen was used to repurify PC-3 cells from MSCs after coculture (not depicted). Levels of phosphorylated Akt (Ser473) in PC-3 cells directly cocultured with MSCs (PC-3 + MSC) were unchanged compared with levels of phosphorylated Akt in PC-3 cells alone (PC-3). In all of the aforementioned experiments, results shown are representative of at least three similar experiments.

0.477 ± 0.05 for KS alone vs. 0.346 ± 0.06 for KS + MSC tumors; $n = 7$ per group; $P < 0.01$). Mirroring our previous in vitro results, we saw no substantial difference in the phospho- to total ERK1 and 2 ratio between lysates from MSC-treated and untreated animals. Immunohistochemical analysis demonstrated that in KS tumors, levels of phospho-Akt were noticeably reduced in the vicinity of incorporated MSCs (Fig. 5 B).

Given the central role of Akt in cell survival and proliferation, particularly in KS cells, we next examined the effect of MSCs on early necrosis within KS tumors. Strikingly, we saw a profound increase in the area of tumor necrosis 7 d after KS tumor implantation and i.v. MSC injection (Fig. 5 C). Using morphometric analysis on multiple sections of KS tumors from treated and untreated animals, we observed a greater than twofold increase in the percentage of tumor that was necrotic in animals treated with MSCs (Fig. 5 D). Similarly, in animals with tumors established before the infusion of MSCs, histological analysis of KS tumors 10 d after the first treatment demonstrated that the MSC-treated animals had smaller nests of viable tumor cells along with a substantially augmented host inflammatory response characterized by a profound neutrophilic infiltrate (Fig. S6, available at http://www.jem.org/cgi/content/full/jem.20051921/DC1).

To further explore the hypothesis that the effect of MSCs on in vivo tumorigenesis depends on Akt inactivation with tumor target cells, we examined the effects of MSCs on PC-3 tumorigenesis in vivo. As noted previously, Akt activity in this tumor cell type was not responsive to MSC inhibition. To test the effects of MSC infusion on PC-3 tumor growth, we implanted 5×10^6 PC-3 cells subcutaneously in athymic nude mice. Half of these mice received 4×10^6 MSCs i.v. on days 0, 3, and 10 after PC-3 tumor implantation, whereas the other half received no further treatment. In contrast to the potent effect on KS tumorigenesis we observed in animals that received multiple dosages of MSCs i.v., treatment with MSCs had no effect on PC-3 tumorigenesis in vivo (Fig. 5 E).

Finally, we asked whether the inhibition of Akt activation was necessary for MSCs to exert their antitumorigenic effect in KS cells. To test this hypothesis, KS cells were transfected with either a constitutively active myristoylated Akt construct (myrAkt; reference 49) or an empty vector control (vector). Tumors from these transfected cells (KS/myrAkt or KS/vector) were implanted 24 h later, and, simultaneously, half of the animals were treated with a single i.v. dosage of 4×10^6 MSCs. As seen in Fig. 5 F, animals receiving KS/myrAkt cells had larger tumors compared with animals receiving KS/vector cells. Consistent with our prior findings, a potent inhibitory MSC effect was once again seen in animals with tumors derived from KS/vector cells. However, we saw no difference in tumor growth with or without MSCs when the KS tumors were engineered to express a constitutively active form of Akt.

DISCUSSION

The aforementioned studies were intended to understand the role of MSCs (the stromal progenitor cell population within the bone marrow) in promoting or inhibiting the growth of a highly angiogenic tumor. As early as 48 h after i.v. injection, MSCs could be observed homing in large numbers to areas of KS tumorigenesis. Our finding that human MSCs home to subcutaneously implanted KS tumors in vitro is consistent with and further strengthens the argument that i.v. delivered human MSCs specifically migrate to sites of active tumorigenesis in vivo. In this regard, it has previously been shown that i.v. injected MSCs can incorporate into tumors within the lung (21). These previous results may need to be interpreted with some caution because we also find that in our model, some MSCs incorporated into the pulmonary microvasculature. As such, MSCs within the pulmonary vasculature may not necessarily represent the direct evidence of tumor-specific homing. In addition to finding cells diffusely scattered throughout the tumor early after injection, we find cells predominantly within the lung as well as within the reticuloendothelial system, with some cells also seen within the bone marrow. Interestingly, we find no evidence of MSCs within other highly vascular organs such as the kidney, heart, and brain. Our observations of the tissue distribution of i.v. injected MSCs are similar to observations of MSC distribution after i.v. injection into animals after myocardial infarction (16). In this previous study, cells were found in the lung, liver, and spleen as well as within the border zone of the infarcted heart. Collectively, these findings suggest that in addition to the reticuloendothelial network, MSCs may have the ability to potentially home to areas of tissue ischemia or active angiogenesis such as the infarcted heart or the tumor microenvironment.

Unexpectedly, we observed a potent inhibitory effect on KS in vivo mediated by human MSCs administered i.v. These effects could be detected early after tumor implantation and cell injection and could be augmented with multiple dosages of MSCs. The inhibitory effects of MSC infusion were demonstrated when MSC infusion began at the time of tumor implantation or when MSCs were used to treat preexisting KS tumors. It is theoretically possible that the delivery of human cells into a mouse inoculated with a human KS tumor might potentiate a nonspecific xenogenic immune response within the mouse that may inhibit in vivo tumorigenesis. Arguing against this possibility is the lack of effect seen when mice are treated with HUVECs, which, like MSCs, are primary human cells that express similar levels of MHC class I and II on their surface. Furthermore, the immune response of the athymic nude mouse, which is mediated primarily by NK cells, is much less vigorous to xenogenic stimuli.

Several of our observations support the argument that human MSCs exert their antitumorigenic effects on KS tumors through direct, local effects on KS cells. In vitro, we see the inhibition of Akt phosphorylation only when the cells are in direct contact. In vivo, we observe very similar effects on cell signaling in tumor lysates of animals that received MSCs. Furthermore, using indirect immunofluorescence, we observe the inhibition of Akt activation in the local microenvironment surrounding the MSCs within KS tumors. Collectively with other studies demonstrating inhibitory effects on dendritic cells (39) and T cells (40), our findings suggest that MSCs can communicate with a variety of cell types and prevent cellular activation in a contact-dependent manner. We extend this work further by demonstrating that the blockade of the adhesion molecule E-cadherin abrogates

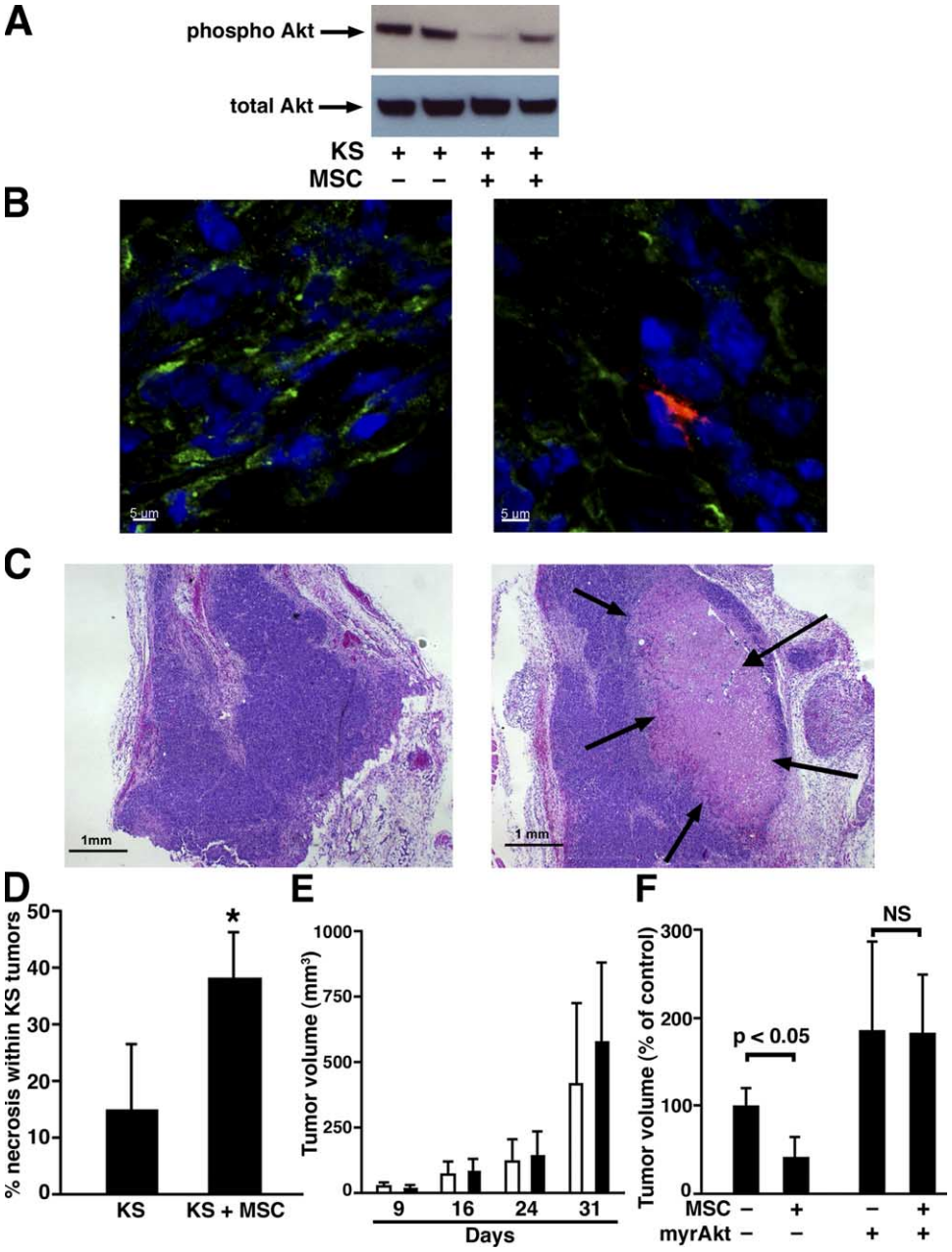

Figure 5. In vivo antitumorigenic effects of MSCs depend on the inactivation of Akt in target tumor cells. (A) Western blot analysis of lysates from four separate tumors harvested on day 2 demonstrates a reduction of phosphorylated Akt (Ser473) in MSC-treated animals. Total Akt levels within tumor lysates are unaffected by i.v. MSC injection. (B) Confocal fluorescence microscopy reveals that in areas surrounding MSCs (red CM-DiI–labeled cell, right), there is diminished phospho-Akt staining (green) compared with an area in the same KS tumor (left) that lacks incorporated MSCs. Cell nuclei are indicated with blue fluorescent DAPI nuclear counterstain. (C) Representative images of day 7 tumors stained with hematoxylin and eosin revealing that tumors from animals receiving i.v. MSCs (right) have more pronounced areas of central necrosis (arrows) compared with tumors from animals receiving no cells (left). (D) Quantitative blinded morphometry of multiple sections in KS tumors demonstrate a greater than twofold increase in the area of necrosis within the tumors in those animals receiving MSCs (KS + MSC) compared with tumors from untreated animals (KS). *, $P < 0.01$; $n = 5$ mice for each group, with at least five random sections per tumor analyzed. (E) On day 0, 5×10^6 PC-3 cells were injected subcutaneously into the posterior right flank of each mouse alone (white bars) or in conjunction with i.v. administration of 4×10^6 human MSCs (black bars). i.v. MSC treatment was repeated on days 3 and 10. Tumor growth and progression were monitored by biweekly caliper assessment (P value is NS on day 31; $n = 5$ per group). (F) On day 0, 5×10^6 KS/vector or KS/myrAkt cells were injected subcutaneously into the posterior right flank of each mouse alone or in conjunction with i.v. administration of 4×10^6 human MSCs. Data are expressed as the percentage of day 23 tumor volume compared with animals that received tumors derived from KS/vector cells alone ($n = 4$ animals for each group). Error bars represent SEM.

the inhibitory effects of MSCs on Akt activation within target cells. Interestingly, the in vivo reduction of phospho-Akt levels within KS tumors appeared to extend to tumor cells that are not in direct contact with incorporated MSCs (Fig. 5 B), suggesting a potential role for paracrine signaling that is initiated after MSC–target cell interaction. The precise molecular details by which contact with MSCs results in the inhibition of Akt activation will be the focus of future work.

Interestingly, we observed that tumors from animals treated with MSCs had a greater proportion of tumor stroma compared with tumors from untreated animals (Fig. S6). The increased fibrous tissue seen within tumors from MSC-treated animals may represent a host response to enhanced tumor necrosis mediated by MSCs. On the other hand, MSCs are known precursors of stromal cells, which generate the extracellular matrix supporting hematopoiesis within the bone marrow microenvironment (50). Therefore, it is possible that within the tumor microenvironment, stromal components derived from MSCs may play a role in inhibiting tumor growth. Detailed characterization of the properties of MSCs after tumor engraftment will be addressed in future studies.

In conclusion, we show that MSCs, a subpopulation of adult bone marrow–derived stem cells, exhibit potent antitumor effects in a model of KS. This effect is mediated by direct cell contact leading to the inhibition of Akt activation within KS cells. These findings contrast with recent studies demonstrating that certain stem cell populations can promote or give rise to neoplastic growth (6, 28, 51). Our findings are particularly surprising in light of the demonstrated proangiogenic effects of MSCs in ischemic tissue (29, 52, 53). Furthermore, our findings suggest that MSCs represent a unique stromal cell population that, in contrast to the reported effects of normal or carcinoma-associated fibroblasts, can directly inhibit tumorigenesis. In light of recent studies demonstrating that infused MSCs may have a therapeutic role in preventing graft versus host disease in cancer patients after bone marrow transplantation (54–56), the antitumorigenic effects of MSCs are particularly reassuring. We speculate that the ability of MSCs to inhibit Akt signaling may also be an important aspect of the endogenous function of MSCs within the normal bone marrow microenvironment. Interestingly, antitumorigenic properties have been previously observed in other microenvironments that support regulated progenitor cell growth and proliferation, such as seen in normal mouse blastocysts (57) or within the cambial layer of tobacco plants (58). Finally, although KS tumors are unique malignancies with an unclear cellular origin, our results suggest at least the potential to exploit the biology of MSCs to treat a subset of human malignancies.

MATERIALS AND METHODS

Primary cells and cell lines. First passage human MSCs obtained from bone marrow aspirates of healthy young donors were purchased from Cambrex. We obtained and pooled MSCs from four different healthy young donors (two male and two female). MSCs were cultured in MSC growth media (MSCGM; Cambrex). Media was changed every 3 d, and cells were split when 70% confluence was achieved. MSCs were used at passage 3–7 for all experiments. HUVECs were also obtained commercially (Cambrex) and were cultured in EGM endothelial cell media (Cambrex). The KS cell line KSIMM was provided by A. Albini (Istituto Nazionale per la Ricerca sul Cancro, Genoa, Italy; reference 59) and was cultured except where indicated in RPMI + 10% heat-inactivated FCS. All coculture experiments were also performed in this media. The human prostate cancer cell line PC-3 and the human breast cancer line MCF-7 were purchased from American Type Culture Collection and were cultured in Ham's F-12K medium with 2 mM L-glutamine + 10% heat-inactivated FCS. Neonatal mouse cardiac myocytes were isolated and cultured as previously described (60).

Cell proliferation measurement. For quantification of KS cells in coculture experiments, KS cells were incubated with CFDA-SE green fluorescent label (Invitrogen) at a final concentration of 5 μM for 15 min and were vigorously washed before coculture. 24 or 48 h after coincubation with human MSCs, KS cell proliferation was quantified using low power epifluorescence microscopy and a hemocytometer (Bright Line; Hausser Scientific). Proliferation experiments were performed with MSCs that were directly cocultured with KS cells or with MSCs separated from KS cells by a transwell membrane with a 0.4-μm pore size (Corning, Inc.). Proliferation experiments were performed in RPMI-1640 media with varying concentrations of FCS ranging from 1 to 10% and either low (1 g/liter) or normal (2 g/liter) glucose concentrations. Proliferation data represent the mean ± SD of triplicate experiments.

Flow cytometry. KSIMM cells that were cocultured with MSCs or HUVECs were harvested 18 h after coculture. Cells were detached with 1 mM EDTA and counted. Cells were prepared for intracellular staining by fixing them in 1% formaldehyde for 10 min at 37°C followed by permeabilization in 90% ice-cold methanol for 30 min. 0.5×10^6 aliquots of cells were washed twice in PBS with 0.5% BSA. Appropriate antibodies were aliquoted into each tube and incubated at room temperature for 30 min. Secondary antibodies conjugated to PE or FITC (Jackson ImmunoResearch Laboratories) were used for the detection of those primary antibodies that were unconjugated. Cocultured cells were also stained with FITC-conjugated Stro-1 antibody (R&D Systems), FITC-conjugated CD31 antibody (BD Biosciences), FITC-conjugated CD44 antibody (BD Biosciences), human prostate cell surface antigen antibody (Chemicon), or FITC-conjugated p185/HER-2 antibody (Biosource International), which enables gating of the MSCs, HUVECS, cardiac myocytes, PC-3 cells, or MCF-7 cells, respectively, and subsequent purification of the KS cells, HUVECs, cardiac myocytes, PC-3 cells, or MCF-7 cells alone. Cells were washed twice in PBS + 0.5% BSA, and samples were subsequently analyzed using a flow cytometer (FACScalibur; BD Biosciences). Antibodies to phospho-Akt (Ser473 and Thr308), Akt, phospho-ERK1/2 (Thr202/Tyr204), and phospho-MEK1/2(Ser217/221) were obtained from Cell Signaling. Appropriate isotype controls were used for each antibody as a control for nonspecific antibody binding. FlowJo software (Tree Star, Inc.) was used to analyze the raw fluorescence-activated cell-sorting data and plot histograms.

Disruption of E-cadherin–mediated interactions in MSC cocultures. For determination of the role of E-cadherin–mediated interactions in KS/MSC or HUVEC/MSC cocultures, a mouse anti–human neutralizing antibody to E-cadherin (Abcam) or an IgG1 isotype control antibody was added at the onset of coculture at a dilution of 1:25. Cocultures were incubated for 18 h in the presence of the E-cadherin neutralizing antibody or IgG1 isotype control, and Akt activation in KS cells or HUVECs was determined by flow cytometry after repurification using techniques described in the previous paragraph.

Animal model. National Institutes of Health Swiss male athymic nude mice (nu/nu) were obtained from the National Cancer Institute (NCI). Animals from age 6 to 10 wk (with no more than a 2-wk spread in a single experiment) were used for tumor formation and inhibition experiments. Animals were housed in micro-isolator cages under sterile conditions and observed for at least 1 wk to ensure proper health before study initiation.

Lighting, temperature, and humidity were controlled centrally and recorded daily. Animals were injected with 5×10^6 KS cells (suspended in 100 μl PBS) subcutaneously into the posterior flanks. Treatment with MSCs or HUVECs was initiated simultaneously or in animals with preestablished tumors by i.v. tail vein injection. In some experiments, mice were given additional doses of MSCs or HUVECs by tail vein injection. Tumors became visible and palpable at day 2 after KS cell inoculation. Tumor growth and progression were monitored by biweekly measurements of tumors with calipers. All mouse experiments were performed using methods described in detailed protocols approved by the Animal Care and Use Committee at the National Heart, Lung, and Blood Institute (NHLBI) and by the Institutional Animal Care and Use Committee at the University of Maryland.

Transfection of KS cells with constitutively active Akt construct. The myristoylated Akt plasmid (myrAkt) has been previously described (49) and was provided by M. Greenberg (Children's Hospital, Boston, MA). KSIMM cells were transfected using the Nucleofector transfection system (Amaxa Biosystems) with myristoylated Akt (KS/myrAkt) or with empty vector (KS/vector). Using a GFP expression vector, we could demonstrate that this strategy routinely resulted in 80–90% transfection efficiencies. 24 h after transfection, KS cells were harvested and washed, and animals were injected with 5×10^6 transfected KS cells (suspended in 100 μL PBS) subcutaneously into the posterior flanks.

Multiplex cytokine measurements. For measurements of cytokine levels from KS cells, MSCs, or HUVECs, we harvested conditioned media 48 h after initial culture, spun down the media to eliminate any cellular material, and snap-froze samples that were stored at −80°C until analyzed. For multiplex cytokine experiments, we used commercially available fluorophore-conjugated bead sets for the following cytokines: ENA-78, G-CSF, IL-1α, IL-6, IL-8, MCP-1, and VEGF-A (all from R&D Systems). Beads were incubated according to the manufacturer's instructions, and data were acquired using a dual-laser instrument (Luminex 100; Luminex Corp.).

Iron labeling of MSCs and in vivo imaging. To label MSCs with superparamagnetic iron oxide particles, MSCs were grown to 70% confluence in MSCGM. MSCs were then washed vigorously and resuspended in a minimal volume of serum-free RPMI-1640 medium (Biosource International). Complexing of polycationic transfection agents to ferumoxides to promote cellular iron uptake was performed as previously described (33). In brief, we used a commercially available ferumoxide suspension (Feridex IV; Berlex Laboratories) in combination with protamine sulfate (American Pharmaceuticals Partner), which was supplied at 10 mg/ml. Ferumoxides were diluted to a final concentration of 100 μg/ml in RPMI-1640 and were combined in a mixing flask with protamine sulfate at a final concentration of 4 μg/ml. The solution containing ferumoxides and protamine sulfate was mixed for 5–10 min with intermittent hand shakings. After 5–10 min, an equal volume of the solution containing FE-Pro complexes was added to the existing media in the adherent cell culture. After incubation for 2–3 h, an equal volume of MSCGM was added to the cells for a final concentration of 25 μg ferumoxides/ml of medium. The cell suspension was then incubated overnight at 37°C. Before injection, cells were vigorously washed twice with PBS plus heparin at 10 U/ml and then twice with ice-cold PBS before being harvested for i.v. injection. Labeling efficiency was >90% and was confirmed by Prussian blue staining of cytospun cell preparations.

MRI was performed using a horizontal bore imaging system (7.0T; Bruker) with 39-G/cm gradients. Mice were anesthetized with 1.5% isoflurane and positioned in a 35-mm Bruker volume coil with physiological monitoring. A water-filled glass tube was positioned adjacent to the tumor site in some mice with small tumors to assist identifying the tumor location. Two-dimensional steady-state gradient echo images were acquired with respiratory gating in coronal and axial planes. Coronal planes were acquired through the body to assess the liver, spleen, marrow, and tumor. Axial planes were acquired to assess the tumor site in detail. In coronal images, imaging parameters were as follows: repetition time/echo time = 550/5.0 ms; nine slices; slice thickness of 0.35 mm; field of view of 5.0×3.0 cm^2; 512×256 matrix; four excitations. For axial images, parameters were as follows: repetition time/echo time = 400/5.0 ms; six slices; slice thickness of 0.35 mm; field of view of 2.5×3.0 cm^2; matrix either of 256×256 or 384×384 zero-filled to 512×512; four to six excitations.

Western blotting. Day 2 tumors were harvested and lysed in lysis buffer (0.5% Triton X-100 in PBS, pH 7.4) with protease inhibitors (complete minileupeptin, aprotinin, and Pefabloc; Boehringer). Protein quantification was performed by bicinchoninic acid assay, and equal amounts of protein lysate were resolved on SDS-PAGE 4–12% gels. Transfer to nitrocellulose membranes was performed in transfer buffer (12 mM Tris base, 96 mM glycine, pH 8.3, and 15% methanol). Membranes were subsequently probed with primary antibodies to phospho-Akt (Ser473) and total Akt (Cell Signaling) and detected using enhanced chemiluminescence (GE Healthcare) according to the manufacturer's protocol.

Microscopy and immunofluorescence. Slides were visualized using wide-field microscopy (both differential interference contrast and fluorescence) using an upright microscope (E-1000; Nikon), and images were acquired on a CCD color digital camera (DXM-1200; Nikon) using ACT1 software (Nikon). To assess the cell localization with higher resolution, images were obtained with a confocal system (SP1; Leica) equipped with UV-Vis lasers (Leica). Images were acquired sequentially using a 351-nm laser line and emission between 420 and 485 nm for DAPI, a 488-nm laser line and emission between 490 and 560 nm for FITC, and a 568-nm laser line and emission between 575 and 690 nm for DiI. Images were obtained with a 63× 1.4 NA plan-Apochromat oil immersion objective (Carl Zeiss MicroImaging, Inc.) using identical hardware settings to allow fluorescence intensity comparisons. Overlay images were assembled, zoomed, and cropped using Imaris 4.1 software (Bitplane).

For immunofluorescence staining, we harvested tumors on day 2 from mice that were killed and immediately perfused with ice-cold saline. Tumor samples were immediately embedded in Tissue-Tek optimal cutting temperature (Sakura Finetek), snap-frozen in isopentane immersed in liquid nitrogen, and stored at −80°C. Cryostat frozen sections were fixed with ice-cold methanol or acetone, blocked for 30 min with 5% goat serum, and incubated overnight at 4°C with a rabbit polyclonal antibody against phospho-Akt (Cell Signaling) at a final dilution of 1:50. To detect evidence of MSC differentiation, we used mouse monoclonal antibodies against human CD13 (1:25), CD33 (1:25), CD34 (1:25), and myeloperoxidase (1:25; Dako-Cytomation). After vigorous washing, sections stained with rabbit antibodies were incubated with a goat anti–rabbit IgG fluorescein-conjugated secondary antibody (Vector Laboratories) at a final dilution of 1:100 at room temperature for 2 h. Antibody detection in sections stained with mouse monoclonal antibodies was performed using the MOM Fluorescein kit (Vector Laboratories). Sections were then washed and coverslipped in Vectashield with DAPI (Vector Laboratories). Parallel samples were incubated with no primary antibody as a specificity control. Normal human blood smears were used as positive control samples for CD13, CD33, and myeloperoxidase staining. MSCs were labeled with the conjugated fluorochrome Cell Tracker CM-DiI (Invitrogen) before i.v. administration for identification in histopathological sections.

Tumor analysis. For measurement of the necrotic area within the tumors, tumors were first harvested and fixed in 10% buffered formalin. Tumors were embedded in paraffin, and serial sections were made at 100-μm increments throughout the tumor. At each level, a section of the tumor was stained with hematoxylin and eosin, and a digital low power photomicrograph was made. Digital images were imported into MetaMorph software v6.1 (Universal Imaging Corp.). The area of necrosis and the total cross-sectional tumor area was identified, traced, and quantified manually. Measurements were performed after masking the treatment allocation group of the given tumor sections. Immunohistochemical staining of KS tumors to determine the presence of host neutrophils within tumors was performed using the rat anti–mouse neutrophil antibody NIMP-R14 (Abcam) at a dilution of

1:25. Antibody detection was performed using the Vectastain ABC kit (Vector Laboratories).

Quantitative phosphoprotein measurements for GSK-3β and ERK1/2 were performed using electrochemiluminescence from Meso Scale Discovery. Day 2 tumors were isolated and snap-frozen. Tumors were thawed and homogenized by sonication within cell lysis buffer containing both phosphatase and protease inhibitors. Protein concentration was measured using the bicinchoninic acid protein assay kit (Pierce Chemical Co.). Equal amounts of protein were input into the assays, and duplicate samples were analyzed from each tumor lysate in triplicate.

Statistical analyses. Statistical analyses were performed using Excel (Microsoft) and Prism 4.0 (GraphPad Software). For tests of comparison, we used a two-sample *t* test. All P values presented are two-tail values.

Online supplemental material. Fig. S1 shows a cytokine profile of MSCs compared with KS cells and HUVECs. Fig. S2 shows a detailed flow cytometric characterization of MSCs. Fig. S3 displays in vivo MRI showing the distribution of iron-labeled MSCs after i.v. injection. Fig. S4 shows that direct coculture of HUVECs with KS cells has no effect on Akt activation in KS cells. Fig. S5 shows that coculture of MSCs with KS cells has no effects on phospho-MEK1/2 levels within KS cells. Fig. S6 shows the comparison of tumors from treated and untreated animals in which tumors were established before the administration of MSCs. Online supplemental material is available at http://www.jem.org/cgi/content/full/jem.20051921/DC1.

We thank Deborah Simon and Mary Angstadt for excellent technical assistance.

This work was supported, in part, by NCI grant 1RO1 CA09905-01 and intramural funds from the NHLBI.

The authors have no conflicting financial interests.

Submitted: 23 September 2005
Accepted: 27 March 2006

REFERENCES

1. Archuleta, T.D., M.P. Devetten, and J.O. Armitage. 2004. Hematopoietic stem cell transplantation in hematologic malignancy. *Panminerva Med*. 46:61–74.
2. Gardner, S.L. 2004. Application of stem cell transplant for brain tumors. *Pediatr. Transplant*. 8:28–32.
3. Smalley, M., and A. Ashworth. 2003. Stem cells and breast cancer: A field in transit. *Nat. Rev. Cancer*. 3:832–844.
4. Scadden, D.T. 2004. Cancer stem cells refined. *Nat. Immunol*. 5: 701–703.
5. Reya, T., S.J. Morrison, M.F. Clarke, and I.L. Weissman. 2001. Stem cells, cancer, and cancer stem cells. *Nature*. 414:105–111.
6. Sell, S. 2004. Stem cell origin of cancer and differentiation therapy. *Crit. Rev. Oncol. Hematol*. 51:1–28.
7. Bhowmick, N.A., E.G. Neilson, and H.L. Moses. 2004. Stromal fibroblasts in cancer initiation and progression. *Nature*. 432:332–337.
8. Bhowmick, N.A., A. Chytil, D. Plieth, A.E. Gorska, N. Dumont, S. Shappell, M.K. Washington, E.G. Neilson, and H.L. Moses. 2004. TGF-beta signaling in fibroblasts modulates the oncogenic potential of adjacent epithelia. *Science*. 303:848–851.
9. Orimo, A., P.B. Gupta, D.C. Sgroi, F. Arenzana-Seisdedos, T. Delaunay, R. Naeem, V.J. Carey, A.L. Richardson, and R.A. Weinberg. 2005. Stromal fibroblasts present in invasive human breast carcinomas promote tumor growth and angiogenesis through elevated SDF-1/CXCL12 secretion. *Cell*. 121:335–348.
10. Barcellos-Hoff, M.H., and S.A. Ravani. 2000. Irradiated mammary gland stroma promotes the expression of tumorigenic potential by unirradiated epithelial cells. *Cancer Res*. 60:1254–1260.
11. Olumi, A.F., G.D. Grossfeld, S.W. Hayward, P.R. Carroll, T.D. Tlsty, and G.R. Cunha. 1999. Carcinoma-associated fibroblasts direct tumor progression of initiated human prostatic epithelium. *Cancer Res*. 59:5002–5011.
12. Javazon, E.H., K.J. Beggs, and A.W. Flake. 2004. Mesenchymal stem cells: paradoxes of passaging. *Exp. Hematol*. 32:414–425.
13. Pittenger, M.F., A.M. Mackay, S.C. Beck, R.K. Jaiswal, R. Douglas, J.D. Mosca, M.A. Moorman, D.W. Simonetti, S. Craig, and D.R. Marshak. 1999. Multilineage potential of adult human mesenchymal stem cells. *Science*. 284:143–147.
14. Hamada, H., M. Kobune, K. Nakamura, Y. Kawano, K. Kato, O. Honmou, K. Houkin, T. Matsunaga, and Y. Niitsu. 2005. Mesenchymal stem cells (MSC) as therapeutic cytoreagents for gene therapy. *Cancer Sci*. 96:149–156.
15. Chen, J., Y. Li, L. Wang, Z. Zhang, D. Lu, M. Lu, and M. Chopp. 2001. Therapeutic benefit of intravenous administration of bone marrow stromal cells after cerebral ischemia in rats. *Stroke*. 32:1005–1011.
16. Barbash, I.M., P. Chouraqui, J. Baron, M.S. Feinberg, S. Etzion, A. Tessone, L. Miller, E. Guetta, D. Zipori, L.H. Kedes, et al. 2003. Systemic delivery of bone marrow-derived mesenchymal stem cells to the infarcted myocardium: feasibility, cell migration, and body distribution. *Circulation*. 108:863–868.
17. Le Blanc, K., C. Tammik, K. Rosendahl, E. Zetterberg, and O. Ringden. 2003. HLA expression and immunologic properties of differentiated and undifferentiated mesenchymal stem cells. *Exp. Hematol*. 31:890–896.
18. Aggarwal, S., and M.F. Pittenger. 2004. Human mesenchymal stem cells modulate allogeneic immune cell responses. *Blood*. 105:1815–1822.
19. Djouad, F., P. Plence, C. Bony, P. Tropel, F. Apparailly, J. Sany, D. Noel, and C. Jorgensen. 2003. Immunosuppressive effect of mesenchymal stem cells favors tumor growth in allogeneic animals. *Blood*. 102:3837–3844.
20. Pittenger, M.F., and B.J. Martin. 2004. Mesenchymal stem cells and their potential as cardiac therapeutics. *Circ. Res*. 95:9–20.
21. Studeny, M., F.C. Marini, J.L. Dembinski, C. Zompetta, M. Cabreira-Hansen, B.N. Bekele, R.E. Champlin, and M. Andreeff. 2004. Mesenchymal stem cells: potential precursors for tumor stroma and targeted-delivery vehicles for anticancer agents. *J. Natl. Cancer Inst*. 96:1593–1603.
22. Cheung, T.W. 2004. AIDS-related cancer in the era of highly active antiretroviral therapy (HAART): a model of the interplay of the immune system, virus, and cancer. "On the offensive–the Trojan Horse is being destroyed"–Part A: Kaposi's sarcoma. *Cancer Invest*. 22:774–786.
23. Reitz, M.S., Jr., L.S. Nerurkar, and R.C. Gallo. 1999. Perspective on Kaposi's sarcoma: facts, concepts, and conjectures. *J. Natl. Cancer Inst*. 91:1453–1458.
24. Ensoli, B., and M. Sturzl. 1998. Kaposi's sarcoma: a result of the interplay among inflammatory cytokines, angiogenic factors and viral agents. *Cytokine Growth Factor Rev*. 9:63–83.
25. Moore, P.S., L.A. Kingsley, S.D. Holmberg, T. Spira, P. Gupta, D.R. Hoover, J.P. Parry, L.J. Conley, H.W. Jaffe, and Y. Chang. 1996. Kaposi's sarcoma-associated herpesvirus infection prior to onset of Kaposi's sarcoma. *AIDS*. 10:175–180.
26. Chang, Y., E. Cesarman, M.S. Pessin, F. Lee, J. Culpepper, D.M. Knowles, and P.S. Moore. 1994. Identification of herpesvirus-like DNA sequences in AIDS-associated Kaposi's sarcoma. *Science*. 266:1865–1869.
27. Serakinci, N., P. Guldberg, J.S. Burns, B. Abdallah, H. Schrodder, T. Jensen, and M. Kassem. 2004. Adult human mesenchymal stem cell as a target for neoplastic transformation. *Oncogene*. 23:5095–5098.
28. Houghton, J., C. Stoicov, S. Nomura, A.B. Rogers, J. Carlson, H. Li, X. Cai, J.G. Fox, J.R. Goldenring, and T.C. Wang. 2004. Gastric cancer originating from bone marrow-derived cells. *Science*. 306:1568–1571.
29. Kinnaird, T., E. Stabile, M.S. Burnett, M. Shou, C.W. Lee, S. Barr, S. Fuchs, and S.E. Epstein. 2004. Local delivery of marrow-derived stromal cells augments collateral perfusion through paracrine mechanisms. *Circulation*. 109:1543–1549.
30. Kinnaird, T., E. Stabile, M.S. Burnett, C.W. Lee, S. Barr, S. Fuchs, and S.E. Epstein. 2004. Marrow-derived stromal cells express genes encoding a broad spectrum of arteriogenic cytokines and promote in vitro and in vivo arteriogenesis through paracrine mechanisms. *Circ. Res*. 94:678–685.
31. Al-Khaldi, A., H. Al-Sabti, J. Galipeau, and K. Lachapelle. 2003. Therapeutic angiogenesis using autologous bone marrow stromal cells: improved blood flow in a chronic limb ischemia model. *Ann. Thorac. Surg*. 75:204–209.

32. Nakamura, K., Y. Ito, Y. Kawano, K. Kurozumi, M. Kobune, H. Tsuda, A. Bizen, O. Honmou, Y. Niitsu, and H. Hamada. 2004. Antitumor effect of genetically engineered mesenchymal stem cells in a rat glioma model. *Gene Ther.* 11:1155–1164.
33. Arbab, A.S., G.T. Yocum, H. Kalish, E.K. Jordan, S.A. Anderson, A.Y. Khakoo, E.J. Read, and J.A. Frank. 2004. Efficient magnetic cell labeling with protamine sulfate complexed to ferumoxides for cellular MRI. *Blood.* 104:1217–1223.
34. Arbab, A.S., L.A. Bashaw, B.R. Miller, E.K. Jordan, B.K. Lewis, H. Kalish, and J.A. Frank. 2003. Characterization of biophysical and metabolic properties of cells labeled with superparamagnetic iron oxide nanoparticles and transfection agent for cellular MR imaging. *Radiology.* 229:838–846.
35. Gullino, P.M. 1976. In vivo utilization of oxygen and glucose by neoplastic tissue. *Adv. Exp. Med. Biol.* 75:521–536.
36. Kwon, S.J., and Y.J. Lee. 2005. Effect of low glutamine/glucose on hypoxia-induced elevation of hypoxia-inducible factor-1alpha in human pancreatic cancer MiaPaCa-2 and human prostatic cancer DU-145 cells. *Clin. Cancer Res.* 11:4694–4700.
37. Pati, S., M. Cavrois, H.G. Guo, J.S. Foulke Jr., J. Kim, R.A. Feldman, and M. Reitz. 2001. Activation of NF-kappaB by the human herpesvirus 8 chemokine receptor ORF74: evidence for a paracrine model of Kaposi's sarcoma pathogenesis. *J. Virol.* 75:8660–8673.
38. Sodhi, A., S. Montaner, V. Patel, J.J. Gomez-Roman, Y. Li, E.A. Sausville, E.T. Sawai, and J.S. Gutkind. 2004. Akt plays a central role in sarcomagenesis induced by Kaposi's sarcoma herpesvirus-encoded G protein-coupled receptor. *Proc. Natl. Acad. Sci. USA.* 101:4821–4826.
39. Beyth, S., Z. Borovsky, D. Mevorach, M. Liebergall, Z. Gazit, H. Aslan, E. Galun, and J. Rachmilewitz. 2005. Human mesenchymal stem cells alter antigen-presenting cell maturation and induce T cell unresponsiveness. *Blood.* 105:2214–2219.
40. Glennie, S., I. Soeiro, P.J. Dyson, E.W. Lam, and F. Dazzi. 2005. Bone marrow mesenchymal stem cells induce division arrest anergy of activated T cells. *Blood.* 105:2821–2827.
41. Birchmeier, W., K.M. Weidner, J. Hulsken, and J. Behrens. 1993. Molecular mechanisms leading to cell junction (cadherin) deficiency in invasive carcinomas. Semin. *Cancer Biol.* 4:231–239.
42. Bosch, F.X., C. Andl, U. Abel, and J. Kartenbeck. 2005. E-cadherin is a selective and strongly dominant prognostic factor in squamous cell carcinoma: a comparison of E-cadherin with desmosomal components. *Int. J. Cancer.* 114:779–790.
43. Motti, M.L., D. Califano, G. Baldassarre, A. Celetti, F. Merolla, F. Forzati, M. Napolitano, B. Tavernise, A. Fusco, and G. Viglietto. 2005. Reduced E-cadherin expression contributes to the loss of p27kip1-mediated mechanism of contact inhibition in thyroid anaplastic carcinomas. *Carcinogenesis.* 26:1021–1034.
44. Pecina-Slaus, N. 2003. Tumor suppressor gene E-cadherin and its role in normal and malignant cells. *Cancer Cell Int.* 3:17.
45. Mangi, A.A., N. Noiseux, D. Kong, H. He, M. Rezvani, J.S. Ingwall, and V.J. Dzau. 2003. Mesenchymal stem cells modified with Akt prevent remodeling and restore performance of infarcted hearts. *Nat. Med.* 9:1195–1201.
46. Shake, J.G., P.J. Gruber, W.A. Baumgartner, G. Senechal, J. Meyers, J.M. Redmond, M.F. Pittenger, and B.J. Martin. 2002. Mesenchymal stem cell implantation in a swine myocardial infarct model: engraftment and functional effects. *Ann. Thorac. Surg.* 73:1919–1925.
47. van Empel, V.P., and L.J. De Windt. 2004. Myocyte hypertrophy and apoptosis: a balancing act. *Cardiovasc. Res.* 63:487–499.
48. Matsui, T., L. Li, J.C. Wu, S.A. Cook, T. Nagoshi, M.H. Picard, R. Liao, and A. Rosenzweig. 2002. Phenotypic spectrum caused by transgenic overexpression of activated Akt in the heart. *J. Biol. Chem.* 277:22896–22901.
49. Dudek, H., S.R. Datta, T.F. Franke, M.J. Birnbaum, R. Yao, G.M. Cooper, R.A. Segal, D.R. Kaplan, and M.E. Greenberg. 1997. Regulation of neuronal survival by the serine-threonine protein kinase Akt. *Science.* 275:661–665.
50. Prockop, D.J. 1997. Marrow stromal cells as stem cells for nonhematopoietic tissues. *Science.* 276:71–74.
51. Singh, S.K., I.D. Clarke, M. Terasaki, V.E. Bonn, C. Hawkins, J. Squire, and P.B. Dirks. 2003. Identification of a cancer stem cell in human brain tumors. *Cancer Res.* 63:5821–5828.
52. Nagaya, N., T. Fujii, T. Iwase, H. Ohgushi, T. Itoh, M. Uematsu, M. Yamagishi, H. Mori, K. Kangawa, and S. Kitamura. 2004. Intravenous administration of mesenchymal stem cells improves cardiac function in rats with acute myocardial infarction through angiogenesis and myogenesis. *Am. J. Physiol. Heart Circ. Physiol.* 287:H2670–H2676.
53. Tang, Y.L., Q. Zhao, X. Qin, L. Shen, L. Cheng, J. Ge, and M.I. Phillips. 2005. Paracrine action enhances the effects of autologous mesenchymal stem cell transplantation on vascular regeneration in rat model of myocardial infarction. *Ann. Thorac. Surg.* 80:229–236.
54. Lazarus, H.M., O.N. Koc, S.M. Devine, P. Curtin, R.T. Maziarz, H.K. Holland, E.J. Shpall, P. McCarthy, K. Atkinson, B.W. Cooper, et al. 2005. Cotransplantation of HLA-identical sibling culture-expanded mesenchymal stem cells and hematopoietic stem cells in hematologic malignancy patients. *Biol. Blood Marrow Transplant.* 11:389–398.
55. Maitra, B., E. Szekely, K. Gjini, M.J. Laughlin, J. Dennis, S.E. Haynesworth, and O.N. Koc. 2004. Human mesenchymal stem cells support unrelated donor hematopoietic stem cells and suppress T-cell activation. *Bone Marrow Transplant.* 33:597–604.
56. Le Blanc, K., and O. Ringden. 2005. Immunobiology of human mesenchymal stem cells and future use in hematopoietic stem cell transplantation. *Biol. Blood Marrow Transplant.* 11:321–334.
57. Mintz, B., and K. Illmensee. 1975. Normal genetically mosaic mice produced from malignant teratocarcinoma cells. *Proc. Natl. Acad. Sci. USA.* 72:3585–3589.
58. Braun, A.C., and H.N. Wood. 1976. Suppression of the neoplastic state with the acquisition of specialized functions in cells, tissues, and organs of crown gall teratomas of tobacco. *Proc. Natl. Acad. Sci. USA.* 73: 496–500.
59. Albini, A., I. Paglieri, G. Orengo, S. Carlone, M.G. Aluigi, R. DeMarchi, C. Matteucci, A. Mantovani, F. Carozzi, S. Donini, and R. Benelli. 1997. The beta-core fragment of human chorionic gonadotrophin inhibits growth of Kaposi's sarcoma-derived cells and a new immortalized Kaposi's sarcoma cell line. *AIDS.* 11:713–721.
60. Hall, G., I.S. Singh, L. Hester, J.D. Hasday, and T.B. Rogers. 2005. Inhibitor-kappaB kinase-beta regulates LPS-induced TNF-alpha production in cardiac myocytes through NF-kappaB p65 subunit phosphorylation. *Am. J. Physiol. Heart Circ. Physiol.* 289:H2103–H2111.